DOI: 10.1002/chem.200800412

Nanoparticle-Based Electrochemical Immunosensor for the Detection of Phosphorylated Acetylcholinesterase: An Exposure Biomarker of Organophosphate Pesticides and Nerve Agents

Guodong Liu,[a, b] Jun Wang,[a] Richard Barry,[a] Catherine Petersen,[a] Charles Timchalk,[a] Paul L Gassman,[a] and Yuehe Lin*[a]

Abstract: A nanoparticle-based electrochemical immunosensor has been developed for the detection of phosphorylated acetylcholinesterase (AChE), which is a potential biomarker of exposure to organophosphate (OP) pesticides and chemical warfare nerve agents. Zirconia nanoparticles (ZrO_2 NPs) were used as selective sorbents to capture the phosphorylated AChE adduct, and quantum dots (ZnS@CdS, QDs) were used as tags to label monoclonal anti-AChE antibody to quantify the immunorecognition events. The sandwich-like immunoreactions were performed among the ZrO_2 NPs, which were pre-coated on a screen printed electrode (SPE) by electrodeposition, phosphorylated AChE and QD-anti-AChE. The captured QD tags were determined on the SPE by electrochemical stripping analysis of its metallic component (cadmium) after an acid-dissolution step. Paraoxon was used as the model OP insecticide to prepare the phosphorylated AChE adducts to demonstrate proof of principle for the sensor. The phosphorylated AChE adduct was characterized by Fourier transform infrared spectroscopy (FTIR) and mass spectroscopy. The binding affinity of anti-AChE to the phosphorylated AChE was validated with an enzyme-linked immunosorbent assay. The parameters (e.g., amount of ZrO_2 NP, QD-anti-AChE concentration,) that govern the electrochemical response of immunosensors were optimized. The voltammetric response of the immunosensor is highly linear over the range of 10 pM to 4 nM phosphorylated AChE, and the limit of detection is estimated to be 8.0 pM. The immunosensor also successfully detected phosphorylated AChE in human plasma. This new nanoparticle-based electrochemical immunosensor provides an opportunity to develop field-deployable, sensitive, and quantitative biosensors for monitoring exposure to a variety of OP pesticides and nerve agents.

Keywords: acetylcholinesterase · immunochemistry · nanoparticles · organophosphate pesticides · sensors

Introduction

Many organophosphates (OPs) are highly neurotoxic because they disrupt the cholinesterase enzyme that regulates the neurotransmitter acetylcholine,[1–5] which is needed for proper nervous-system function. There are at least 13 types of OPs and hundreds of OP compounds in use, which are derivatives of phosphoric, phosphonic, or phosphinic acids.[6] Most are used as pesticides, but a few have been used as chemical weapons. After the tragic events of September 11, 2001, the perceived threat of a chemical attack by terrorists has emphasized the need for effective countermeasures that can rapidly diagnose and mitigate the effects of highly toxic chemical exposures.[7,8] In general, a definitive diagnosis of pesticide or nerve-agent exposure is required for the initiation of appropriate medical countermeasures, whether exposure is a result of chemical attack, accident, or self-inflicted.[9] In addition, confirmation of exposure to nerve agents is important for the health surveillance of persons handling such agents for use as pesticides or as an indicator of illegal

[a] Dr. G. Liu, Dr. J. Wang, Dr. R. Barry, Dr. C. Petersen, Dr. C. Timchalk, P. L. Gassman, Dr. Y. Lin
Pacific Northwest National Laboratory
Richland, WA 99352(USA)
Fax: (+1) 509-376-5106
E-mail: guodong.liu@ndsu.edu
yuehe.lin@pnl.gov

[b] Dr. G. Liu
Department of Chemistry and Molecular Biology
North Dakota State University, Fargo, ND 58105 (USA)

Supporting information for this article is available on the WWW under http://dx.doi.org/10.1002/chem.200800412.

activity or for forensic purposes (e.g., verification of an alleged use of nerve agents). Finally, the verification of non-exposure to nerve agents is of great importance to concerned individuals.[10]

Following OP exposure in humans or animals the agent can exist in several forms including: phosphyl-enzyme complexes and protein adducts, unbound nerve agent, and hydrolysis products (phosphonic acids). Figure 1 represents the

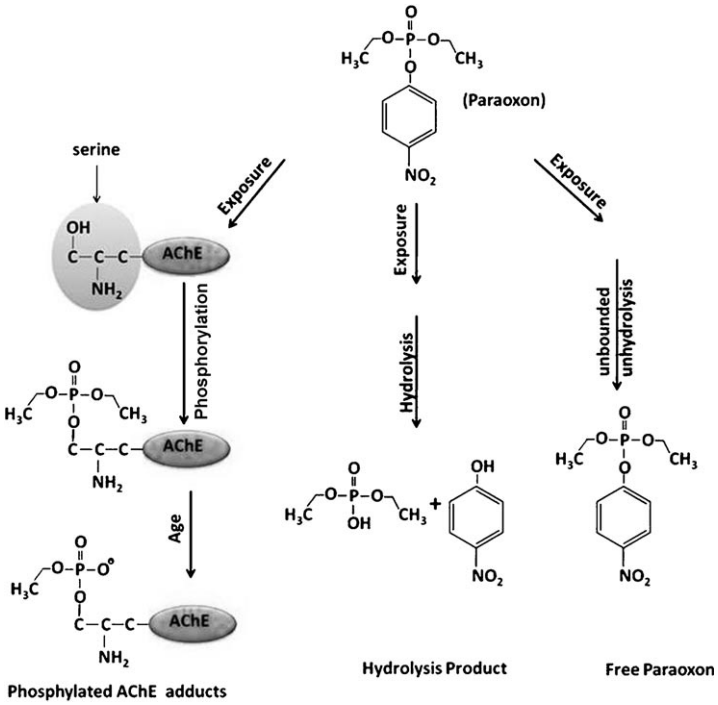

Figure 1. Various reaction paths of paraoxon after systemic exposure.

biological fate of OPs (paraoxon as model compound) within the human body. Organophosphates covalently bind to several essential enzymes including: acetylcholinesterase (AChE), butyrylcholinesterase (BChE), serine esterase, carboxylesterase (CaE), neuropathy target esterase (NTE), trypsin, and chymotrypsin.[11–16] Furthermore, binding to a tyrosine residue of human serum albumin has been observed.[17] The persistence of unbound OPs in the body is dependent on their physical-chemical properties and the activity of endogenous organophosphorus hydrolyzing enzymes.[18] However, the high reactivity of these agents with biological targets suggests that levels of unbound OP will be small. Chemical or enzymatic decomposition of OPs results in the formation of inactive phosphonic acids that are renally excreted.[19]

In view of the fate of OPs in biological systems, different analytical methods and technologies have been used to diagnose and retrospectively verify exposure to these nerve agents. These methods include: a modified Ellman colorimetric assay for cholinesterase activity,[20–22] identification and quantification of unbound nerve agent,[23] analysis of decomposition products by gas chromatography-mass spectrometry (GC-MS)[24] or liquid chromatography-mass spectrometry (LC-MS)/MS,[25,26] fluoride-induced reactivation of inhibited AChE and BChE with reconstitution of the inhibitor and analysis by GC-MS,[27] and analysis of phosphyl-protein-adducts in plasma by capillary electrophoresis-MS and LC-MS/MS.[28–30] Of the approaches listed above, the colorimetric assay remains a mainstay for the fast initial screening of OP exposure, but it lacks sensitivity and specificity, and control (or baseline) levels of cholinesterase activity must be obtained from each subject before analyzing OP exposure.[31] Mass spectrometry (MS) in connection with other separation and detection technologies has been widely used for detecting hydrolysis products, unbound nerve agents, and phosphorylated cholinesterase adducts in biological matrixes, such as red blood cells, plasma, and urine. MS methods provide very good sensitivity and accuracy, but are currently limited to laboratory analyses given the requirement for sophisticated and expensive equipment. Hence, rapid, sensitive, and field-deployable methods are still needed, and new or improved diagnostic techniques or tools that can provide rapid and reliable evaluation of nerve-agent exposure will enhance our ability to respond quickly to an emergency and thus improve our ability to medically counteract the effects.

Electrochemical immunoassays and immunosensors have evolved dramatically over the past two decades and are ideally suited for meeting the portability requirements of decentralized point-of-care testing or field detection of chemicals agents.[32] Recently, nanomaterial-based electrochemical immunoassays and immunosensors have attracted considerable interest given the potential for developing selective and sensitive miniature diagnostic tools.[33–34] In this paper, we demonstrate initial work toward developing a highly selective, ultrasensitive, and disposable immunosensor that can detect sub-clinical exposure to OPs by using nanoparticle-linked antibodies and metal chelation to selectively capture phosphorylated AChE biomarkers followed by electrochemical detection. Proof of principle is exhibited by detection of organophosphate-modified human AChE in vitro.

Results and Discussion

Preparation and characterization of phosphorylated AChE adducts: The biochemical mechanism of OP and inactivation of AChE is a widely accepted process and is initiated by precursory phosphorylation at the catalytic serine residue.[35] In this study, paraoxon was used as a model of OP pesticide and nerve agent to prepare diethylphosphoryl protein adducts for the development of an electrochemical immunosensor. The diethylphosphoryl adduct can then undergo aging and result in the loss of an alkyl group, leading to the formation of monoethylphosphoryl adduct. Historically, alkylphosphoryl adducts of ChE are simply referred to as phosphorylated ChE. In our study, the phosphorylated AChE adduct was prepared by adding freshly prepared paraoxon solution (in acetone) to the purified human AChE

(from red blood cells) in a tris-HCl buffer (pH 8.0) at a molar ratio of 1.8:1 (paraoxon to AChE). The enzyme activity was measured with the modified Ellman colorimetric method. The decrease in the AChE activity was monitored until inhibition was complete. It was found that the AChE activity decreased as a function of contact time, with nearly complete enzyme inhibition being achieved within two hours (Figure S1,Supporting Information). These results were then used as the basis for all subsequent in vitro paraoxon-AChE experiments.

FTIR spectroscopy and MS was used to confirm formation of the phosphorylated AChE adduct. The infrared spectra of paraoxon, AChE, and phosphorylated AChE adduct were recorded (Figure 2). Strong absorption bands resulting from O–C–C stretching ($\tilde{\nu}=1022$ and 921 cm^{-1}) are exhibited in the spectra of paraoxon and phosphorylated AChE, but absent in the spectrum of AChE alone. In addition, several bands associated with the nitrophenyl leaving group of paraoxon were absent upon formation of the diethylphosphoryl adduct on AChE: C=C stretching associated with conjugated double bonds and absorption bands of aryl-NO_2 (Figure 2). Consistent with our understanding of OP to AChE inhibition and FTIR analysis, the formation mechanism of phosphorylated AChE is illustrated in Figure 1 (left side). The phosphorylation of AChE by paraoxon is synchronous with the release of *p*-nitrophenoxy (-$OPhNO_2$) to yield a stable, covalent diethylphosphoserine ester bond at the active site serine (S234). The phosphorylated AChE can usually undergo two possible post-inhibition fates, reactivation or "aging." The reactivation process occurs by cleavage of the phosphoester-serine bond, either spontaneously (water) or mediated by oxime antidotes. The "aging" process occurs when a phosphoester bond other than phosphoserine is cleaved to produce a phosphate oxyanion; in this case, the modification at the active site serine, diethylphosphoserine, ages to become monoethylphosphoserine, a negatively charged anion at neutral pH. The "aged" phosphorylated AChE adduct is considered an irreversible inhibition and the enzyme remains inactive.

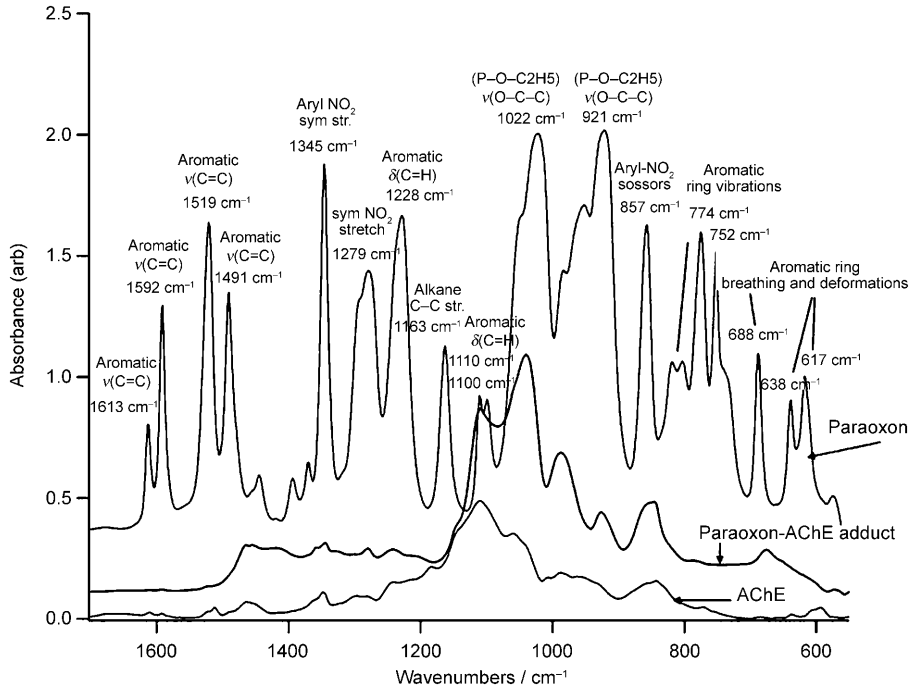

Figure 2. Typical FTIR spectrums of paraoxon, AChE, and paraoxon-AChE adduct.

LC MS/MS analyses confirmed the generation of OP adduct. Paraoxon-modified huAChE (P22304) was chemically cleaved with CNBr followed by chymotrypsin proteolysis and analyzed with nanoLC-ion trap MS/MS (see methods below). The use of CNBr allowed for efficient initial cleavage of huAChE in the presence of the glycoinositol phospholipid membrane anchor for the erythrocyte associated protein, whereas chymotrypsin generated smaller peptides, which are ideal for MS/MS sequencing. Using MASCOT, 68% of the protein was detected and characterized for post-translational modification (Figure S2, Supporting Information). Generation and confirmation of monoethylphophorylated (aged) AChE was confirmed at the active site serine (S234) by detection of peptide 222–242, GGDPTpSVTLFGESAGAASVGMh ($M_r=1987.88$), and subsequent neutral scan loss of the fragmented peptide as assigned by b- and y-ions (Figure 3, Table S1). This peptide was further confirmed by identification of internal fragments 4–10 (In4–10). Including the overall, eighteen daughter ions from the CID spectrum were confidently assigned and an ion score of 24 was obtained for the b- and y-ion assignment alone. Although there are three serines in this peptide, only modification of the active site serine is known to cause enzyme inhibition, and therefore the modification is assigned accordingly. In addition, we believe this is the first full LC MS/MS characterization of huAChE from red blood cells to be published (i.e., non-recombinant human red blood cell AChE).

QD based electrochemical immunosensing mechanism: Recent studies in our group and others have shown that zirconium oxide (ZrO_2) nanoparticles can selectively capture OPs, pesticides, and phosphorylated peptides because of the strong affinity of ZrO_2 for the phosphoric group.[36,37] The principle of immunosensing phosphylated protein biomarkers is similar to traditional sandwich immunoassays except that primary recognition is performed by ZrO_2 nanoparticle

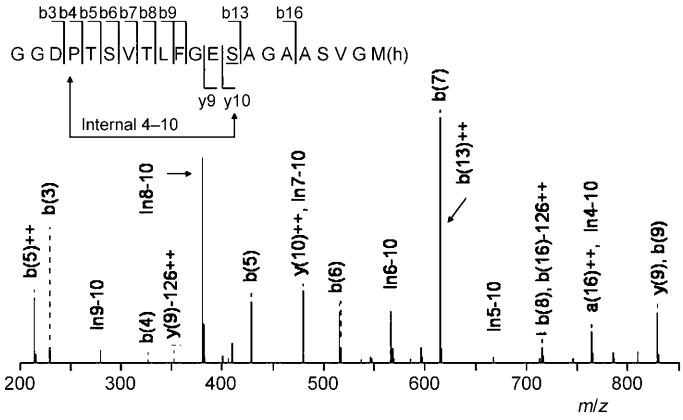

Figure 3. Mass spectrum of collision-induced dissociation of the 4+ ion, 497.76, from LC-MS/MS analysis of alkyphosphorylated AChE, retention time 4.6 min. Assignment of the resulting fragments peaks (daughter ions) can be confidently assigned to b- and y-ions and internal fragmentation of a subpeptide of the 21 amino acid sequence GGDPTSVTLFGE-SAGAASVGMh (peptide 222–242) with a homoserine C-terminus (Mh, due to incubation with CNBr). Assignments made from the amino terminus of the parent peptide (far left, G) begin with b1 through b21 (left to right), whereas those that begin from at the carboxyl terminus (far right, Mh) are numbered y1 and through y21 (right to left). Each experimental peak mass that can be matched to a subsection of the parent peptide is labeled in the spectrum and the corresponding amino acid sequence for the fragment is shown in the upper left of the figure. For example, b7 has a mass of 614.28 (Table S1) and is assigned to GGDPTSV. Using the MASCOT sequence mapping algorithm, an ion score greater than13 indicates identity or extensive homology at $p<0.05$; a score of 24 was obtained here. The match is further confirmed by detection of internal fragments 4–10 (In4–10, PTSVTLF). Most importantly, a monoethyl-phosphoryl mass adduct of 107.998 Da is included in the assignment of y9, the doubly charged y10++, doubly charged a16++, and y9–126 (neutral loss of monoethylphosphate, $M_r=126.01$ from y9); the overlap of these sequences pinpoints the OP adduct to Ser 13 within the parent peptide (from left to right). In addition, only modification of active site serine S234 (amino acid S13 of this peptide) by alkyphosphorylation is known to yield inactive AChE as demonstrated by our Ellman assay.

chelation with the phosphorylated moiety of phosphylated protein. Secondary recognition is performed by QD-tagged anti-AChE antibodies. Figure 4 schematically illustrates the procedure of electrochemical immunosensing of phosphorylated AChE adduct based on a QD label and a ZrO_2 nanoparticle-modified screen printed electrode (SPE). The phosphorylated AChE is first captured by the ZrO_2 nanoparticles. The QD-tagged anti-AChE conjugate is introduced to form the sandwich-like complex on the sensor surface. The captured QDs are then dissolved by a drop of acid to release cadmium ions. This is followed by square-wave voltammetric (SWV) detection of the released cadmium ions at an in situ plated mercury film electrode. In this protocol, the use of ZrO_2 nanoparticles to capture the phosphorylated AChE avoided the use of a capturing antibody, which would need to be specific against the phosphorylated AChE adduct and is currently not commercially available.

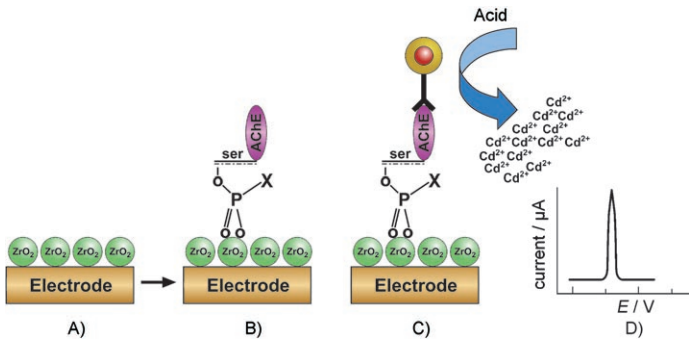

Figure 4. The principle of electrochemical immunosensing of phosphorylated AChE, A) ZrO_2 nanoparticle modified SPE; B) selective capturing phosphorylated AChE adducts; C) Immunoreaction between bound phosphorylated AChE adducts and QD-labeled anti-AChE antibody; D) dissolution of nanoparticle with acid following an electrochemical stripping analysis. AChE: purple, ZnO_2: green, electrode: yellow.

Evaluation of binding affinity of anti-AChE antibody to phosphorylated AChE adduct: A monoclonal anti-AChE antibody was purchased from Abcam (Cambridge, MA) and the manufacturer instructions stated that it is specific to human AChE. However, it was not clear whether this monoclonal antibody would also recognize phosphorylated AChE. We studied its binding affinity using a traditional enzyme-linked immunosorbent assay (ELISA). The monoclonal anti-AChE was conjugated with horseradish peroxidase (HRP) for ELISA application. Purified AChE and phosphorylated AChE were used as targets. The details are explained in the experimental section. Good responses were observed for both AChE and phosphorylated-AChE (Figure S3, Supporting Information). Thus, the monoclonal anti-AChE antibody has good affinity for both native and phosphorylated AChE. On the other hand, a significantly low response was observed in the control experiment using bovine serum albumin (BSA) as a target. This preliminary result demonstrates that the monoclonal anti-AChE antibody can be used for the development of an immunosensor for detection of phosphorylated AChE.

The monoclonal anti-AChE was thus conjugated with QD tags for the development of electrochemical immunosensors based on ZrO_2-coated SPE. First, we investigated the binding affinity of QD-tagged anti-AChE to phosphorylated AChE with the proposed electrochemical immunosensing approach (atop ZrO_2-coated SPE). Table 1 shows the typical electrochemical responses of phosphorylated AChE, purified AChE, a mixture of phosphorylated AChE and AChE, as well as BSA control on the immunosensors.

Theoretically, minimal absorption of AChE and BSA on the ZrO_2 SPE will occur, while strong absorption of phosphorylated AChE is expected. Subsequent detection of ZrO_2 captured material with the electrochemical detection of QD-tagged antibody generated a well-defined voltammetric peak current of 530 nA (peak potential of −0.78 V) from stripping voltammetric detection of the cadmium component of the QDs. Much lower responses (20 and 10 nA) were observed in the control experiments of purified AChE and nonspecific protein BSA, respectively. Signals from the control experiments are ascribed to the nonspecific adsorption of QD-anti-AChE on the SPE surface. Such signal differen-

Table 1. Electrochemical responses of various species on immunosensor.[a]

Sample	Concentration [nM]	Electrochemical responses [nA]
phosphorylated AchE	1.0	530
AchE	5.0	20
BSA	5.0	10
phosphorylated AchE + AChE	1.0 + 5.0	480

[a] Immunoreaction time: 1 h; QD-Ab conjugate (10 μL, 1/20, v/v) was used during the incubation. [b] SWV measurements were performed by using an in situ plated Hg film on the SPE by a 2 min accumulation at −1.4 V. Subsequent stripping was performed after a 2-second rest period from −1.0 V to −0.5 V with a step potential of 4 mV, amplitude of 25 mV, and frequency of 5 Hz.

ces between the phosphorylated AChE and controls (AChE and BSA) suggest preferential formation of ZrO_2- phosphorylated AChE -anti-AChE-QD complexes. Since a mixture of both AChE and phosphorylated AChE is to be expected in real biological samples at low levels of exposure, a mixture of AChE and phosphorylated AChE was examined as a sample to challenge our proposed approach. We obtained an electrochemical response of 480 nA for the mixture which is slightly lower than that of phosphorylated AChE alone (530 nA), indicating that co-existing AChE does not adversely affect the electrochemical response of the immunosensor.

Optimization of the parameters for electrochemical immunosensing phosphorylated AChE adduct: The principle of the proposed electrochemical immunosensor is based on a sandwich-like immunoreaction on the ZrO_2-coated SPE. ZrO_2 nanoparticles are used as a capturing platform and immobilized on the SPE surface to capture the phosphorylated AChE moiety. The amount of ZrO_2 immobilized influences the amount of phosphorylated AChE bound to the surface of the immunosensor, and this accounts for the amount of QD-anti-AChE. Figure 5A displays the response current as affected by the amount of ZrO_2, which was controlled by changing the cyclic voltammetric scanning cycles during the preparation of ZrO_2-coated SPE. The response current increases upon raising the cyclic voltammetry (CV) cycles from 2 to 10, and then it starts to decrease. Ten cycles of CV scanning were used to prepare the electrode for the following experiments. The decrease in current at higher amounts of ZrO_2 (more cycles) may be attributed to an increase in electrode resistance, which decreases the sensitivity of metal ion measurement.

Nonspecific adsorption is one of the important issues in the development of nanoparticle-tag-based biosensors and bioassays. In the current study, there was an electrochemical response obtained from the control sample (in the absence of phosphorylated AChE; see Table 1). This is due to nonspecific adsorption of QD-anti-AChE conjugate on the sensor surface. To minimize such nonspecific adsorption, we found that adding 0.5% BSA in the QD-anti-AChE conjugate solution and blocking the electrode surface (after capturing paraoxon-AChE) with 1% BSA significantly decreased nonspecific adsorption. Figure 5B presents the electrochemical responses of the sensors to 0.5 nM (sample) and 0 nM (control) phosphorylated AChE in the absence and presence of BSA. Although the electrochemical signals of both the sample and control decreased after using BSA as a blocking agent, the signal to background ratio was improved more than three times. A negligible signal was observed from the control sample. Limiting of nonspecific adsorption may be attributed to a shielding effect of BSA when adsorbed on the surface of the QD and the sensor surface.

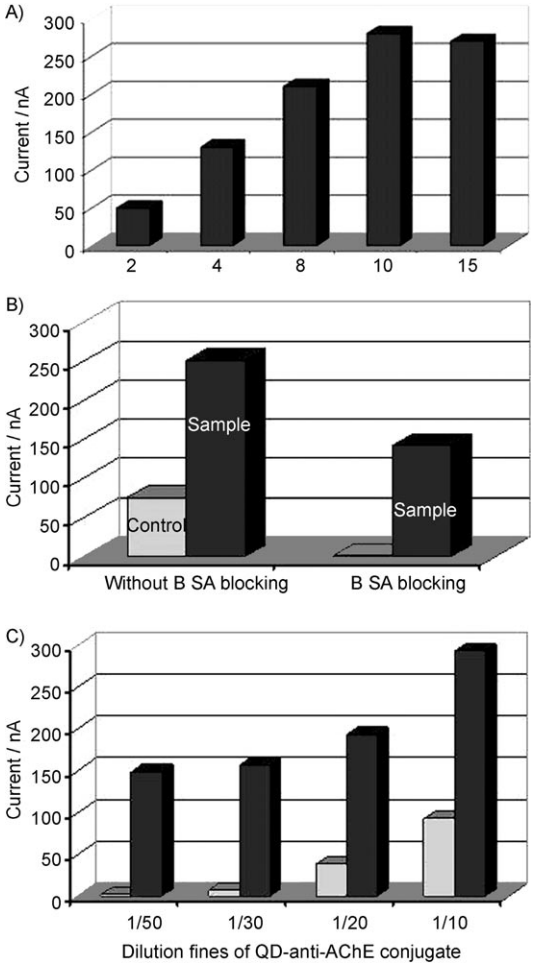

Figure 5. A) The effect of the amount of ZrO2 on the response of the immunosensor; the amount of ZrO2 was controlled by the cycles of cyclic potential scanning; B) BSA block effect on the immunosensor responses; C) the effect of QD-anti-AChE concentration; concentration of phosphorylated AChE: 0.5 nM. The conditions of electrochemical measurement are the same as in Table 1.

The response signal of the immunosensor depends on the amount of QD-anti-AChE conjugate bound to the phosphorylated AChE on the surface of the ZrO_2-coated electrode. The optimal amount of QD-anti-AChE in the incubation solution was determined by incubating the phosphorylated AChE captured sensors with different concentrations of QD-anti-AChE solution, which were prepared by diluting the original conjugate solution. Figure 5C presents the electrochemical responses of the sensors to 0.5 nM (sample) and

0 nM (control) of phosphorylated AChE with different concentrations of QD-anti-AChE. Electrochemical responses of samples and controls increase with increasing concentration of conjugate. The optimum ratio of the sample to control was obtained at the 1/50 dilution. So a 1/50 dilution of the conjugate solution was used in most experiments.

Performance of the immunosensor: Under optimal experimental conditions, we examined the performance of the immunosensor with different concentrations of phosphorylated AChE. Figure 6 displays typical electrochemical responses of the sensor with increasing concentrations of phosphorylated AChE from 10 pM to 4 nM. Well-defined stripping voltammetric peaks (from cadmium ions) are observed across the concentration range. The peak current intensities increase with increasing phosphorylated AChE concentrations. The resulting calibration plot of current versus known concentration of phosphorylated AChE (Figure 6 inset, bottom) is linear over the 10 pM to 4 nM range and is suitable for quantitative work. Also shown in Figure 6 top inset are the SWV signals for a 10 pM phosphorylated AChE sample and 0 pM control, respectively. A small signal was observed in the control experiment (in the absence of phosphorylated AChE). Such behavior is ascribed to the blocking step with 1% BSA. The response of 10 pM phosphorylated AChE indicates a detection limit of 8 pM (based on $S/N=3$), which is comparable to that of mass spectrometric analysis of phosphylated cholinesterase adducts.[28] A series of six measurements of 100 pM phosphorylated AChE yielded reproducible electrochemical responses with an RSD of 4.3% (data not shown). The target application of the immunosensor developed in this work is for biomonitoring of low-dose OP exposure level (<15% inhibition of plasma cholinesterase). At such exposure level, the victims will not show acute symptoms but may have a harmful biological effect. The average AChE level at human plasma is around 8.0 ng mL^{-1} ($\approx$0.12 nM).[35] Based on a simple calculation, the OP-AChE level in human plasma is around 0.018 nM for the low-dose exposure victims. Therefore, the immunosensor developed from this work should have the sensitivity for biomonitoring of low-dose exposure to OPs.

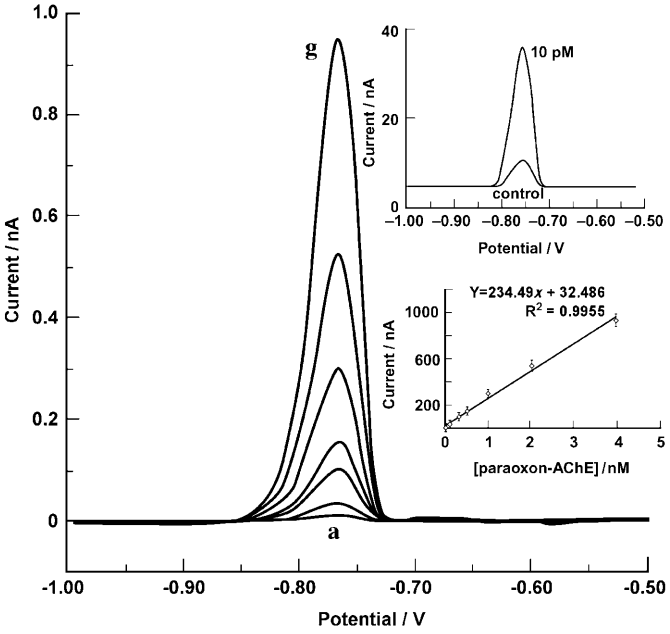

Figure 6. Typical electrochemical responses of the immunosensor with the increasing phosphorylated AChE concentration (0.01, 0.05, 0.3, 0.5, 1.0, 2.0, 4 nM from a to g). The insets show the resulting calibration plot (bottom) and the electrochemical responses of 10 pM and 0 pM (top) paraoxon-AChE. Each concentration was measured three times with three different immunosensors. The immunoreaction time was 1 hr; 10 μL of QD-Ab conjugate (1/50, v/v) was used during the incubation. Electrochemical measurement conditions were the same as in Table 1.

Analysis of phosphorylated AChE in spiked human plasma samples: To explore the use of the biosensor for monitoring biological matrices, human plasma samples (Golden West Biologicals) were spiked with phosphorylated AChE to final concentrations of 25 and 80 pM. Plasma control samples without the addition of phosphorylated AChE were also evaluated. Analysis of 50 μL of sample was performed using the immunosensor. Phosphorylated AChE concentrations of the spiked samples were quantified based on the peak current intensity generated from the samples and the calibration curve depicted in Figure 6. As shown in Table 2, the recoveries for these spiked samples obtained from the immunosensor are calculated to be between 106% and 109%. A more rigorous analysis of the analytical performance of the immunosensor for use with biological matrices is underway; however, these preliminary results demonstrate the potential for characterizing very low levels of OP exposure using biological matrices.

Table 2. Electrochemical immunosensing of phosphorylated AChE in human plasma.[a]

Sample	Response current [nA]	Phosphorylated AChE [pM][b]	Recovery [%]
Human plasma	6.1	ND	N/A
Human plasma + 25 pM Posphoylated AChE	38.7 ± 0.8	26.5 ± 3.4	106
Human plasma + 80 pM Phosphorylated AChE	52.4 ± 1.1	87.2 ± 2.6	109

[a] samples were prepared by spiking purified phosphorylated AChE in human plasma. [b] The concentration of the spiked phosphorylated AChE was calculated by the obtained electrochemical response and the calibration curve depicted in Figure 6. Each sample was measured three times with three different electrodes.

Conclusion

We have presented a nanoparticle-based electrochemical immunosensor with the potential to measure phosphorylated AChE as a biomarker of OP exposure. Under optimal conditions, the immunosensor is very sensitive with the detection limit of 8.0 pM. Further, we have demonstrated the use

of the sensor to detect phosphorylated AChE in complex biological matrices with satisfactory results. Other transitional metal oxide such as titanium oxide has also been used as capturing agents for OPs. TiO_2 is generally used as a capturing agent for photocatalytic decomposition of OPs.[23] OP-specific antibody is a good capturing agent for developing immunoassay methods for detection of protein -OP adducts. However, the rare commercial availability of these specific antibodies limits the development of antibody-based methods. Because of the ease of fabrication and its high affinity to OPs, ZrO_2 as capturing agents shows promising for developing a portable and sensitive detector for measurement of protein-OP adducts. The developed immunosensor represents a new sensitive and quantitative tool for potentially monitoring for a wide variety of OP exposures. Simultaneous detection of multiple phosphorylated esterase adducts could be realized by using different metallic nanoparticle tags, such as CdS and PbS and specificity/selectivity could be improved by using an QD-tagged anti-phosphorylated ChE antibody. Replacement of toxic metals (cadmium and mercury) with environmentally friendly bismuth and antimony would further enhance the power of the new protocol.[38,39] Current research is being performed in these areas as well as further validating the performance of these devices and fabrication of an affordable disposable version.[34c] Overall, the immunosensor presented here shows great promise for in-field and point-of-care diagnosis of OP pesticides and nerve-agent exposures.

Experimental Section

Reagents: Paraoxon, non-recombinant human AChE from red blood cells, acetylthiocholine iodide, zirconium oxychloride ($ZrOCl_2$), 1-ethyl-3-(3-dimethylaminopropyl)carbodiimide hydrochloride (EDC), hydroxylamine, CNBr, alpha-chymotrypsin (type I-S), 2-mercaptoethanol, *N*-hydroxysuccinimide (NHS), 2-(*N*-morpholino)ethanesulfonic acid (MES) buffer, horseradish peroxidase (HRP) and 5,5-dithio-bis(2-nitrobenzoic acid) were purchased from Sigma–Aldrich. Polyclonal and monoclonal anti-AChE antibodies were purchased from Abcam. A Qdot@655 antibody conjugation kit was purchased from Invitrogen. Human plasma was purchased from Golden West Biologicals. Other reagents were commercially available and were of analytical reagent grade. Solutions were prepared with ultrapure (18 MΩ) water from a Nanopure purification system (Billerica, MA).

Instruments: Square-wave voltammetric (SWV) measurements were performed using an electrochemical analyzer CHI 660 (CH Instruments, Austin, TX) connected to a personal computer. A disposable screen-printed electrode (SPE) consisting of a carbon working electrode, a carbon counter electrode, and an Ag/AgCl reference electrode was purchased from Alderon Biosciences, Inc. for electrochemical measurements. A sensor connector (Alderon Biosciences) allows for connecting the SPE to the CHI electrochemical analyzer. LC MS/MS analyses of the phosphorylated AChE was performed using the Agilent 1200 series LC system, Agilent HPLC-Chip cube and Agilent 6330 XCT ion trap. Centrifugal filter devices (AmiconUltra-15, 30000 MWCO, Millipore Corporation) were used to separate and concentrate the sample solution. Dialysis was performed with Float-A-Lyzer (MWCO 25 000, Spectrum Laboratories). The Disposable PD-10 desalting column packed with Sephadex G-25 medium (exclusion limit 5000) was purchased from Amersham Bioscience Corporation and used to purify the protein solution. Centrifugation was performed with a Sorvall RC 26 plus (Kendro Laboratory Product).

Preparation of phosphorylated AChE adducts: AChE was diluted in phosphate buffer (0.01 M, pH 7.4, final concentration, 110 nM) before paraoxon addition. Paraoxon was diluted in an appropriate vehicle, such as acetone, at less than 5% of the total volume and had no significant effect on AChE activity or reactivity with anti-AChE. The final concentration of paraoxon was 750 μM. AChE was incubated with paraoxon for 2 h at room temperature. The decrease in enzyme activity was monitored until inhibition was complete. The solution was dialyzed against phosphate buffer (0.01 M) with saline (PBS) (2×1 L) overnight at 4 °C, to remove the excess of paraoxon. Finally, a volume of phosphorylated AChE was decreased to approximately 0.4 mL by ultrafiltration (Millipore Ultrafree-MC, Bedford, MA). The protein content of the concentration was determined spectrophotometrically at $\lambda = 280$ nm using an absorption coefficients of $E^{1\%} = 16$.

Preparation of phosphorylated AChE samples for mass spectrometry (MS) analysis: Prior to the MS characterization, phosphorylated AChE was precipitated with ice-cold acetone (1:4 vol/vol), the acetone was decanted, and the remaining pellet dried in a speed-vac. The pellet was resolubilized in of degassed HCl (100 μL, 0.1 N) and CNBr (2.5 μL of 20 nmol μL^{-1}) was added (a 20-fold excess) to chemically cleave the lipophilic protein at the C-terminus of methionine residues for 12 h at room temperature, in the dark. CNBr was removed by adding acetonitrile (200 μL) and lyophilizing the sample to dryness in a speed-vac. Finally, the pellet was resolubilized in ammonium bicarbonate (200 μL, 50 mM, pH 7.8) and treated with chymotrypsin (10 μL, 0.1 μg μL^{-1}) at a protein to enzyme ratio of 1:20 for 12 h, at 37 °C. Proteolysis was stopped by flash freezing at −80 °C.

Mass spectrometry analyses: LC MS/MS analyses of the huAChE peptides was performed by using the Agilent 1200 series LC system, Agilent HPLC-Chip cube and Agilent 6330 XCT ion trap. 100 nL of peptide solution were loaded onto a 4 mm, 40 nL enrichment column and separated on a polymer embedded 75 μm×43 mm column containing 5 μm, 300 Å ZORBAX SB-C18. The mobile phases employed were: 0.1% formic acid in water (A phase) and 90% acetonitrile with 0.1% formic acid (B phase). After initial loading at 3% B, the gradient increased to 70% B over 10 minutes then ramped to 95% B in two minutes. The analytical flow rate was 600 nL min^{-1}. Peptides were ionized using nano-electrospray in the positive mode and automatically detected in MS/MS mode from 50–2200 m/z. Peptide mass mapping of MS/MS data was performed using MASCOT® (MatrixScience) after configuring the "enzyme file" to include a CNBr/Chymotrypsin cleavage and configuring the "modifications file" to include the following variable modifications: homoserine and homoserine lactone at C-terminal methionines, diethylphosphorylation (DEP) of serine with neutral scan loss of 154.0395 (monoisotopic), and monoethylphosphorylation of serine (which results from "aging" of the DEP adduct) with a neutral scan loss of 126.0082 (monoisotopic).

AChE and phosphorylated AChE activity assay: A modified Ellman assay was performed essentially as described.[20] AChE or phosphorylated AChE was diluted serially in 0.1 M phosphate buffer (pH 7.4) and 2 μL added to a microtiter plate. The plate substrate acetylthiocholine iodide (ATCh-I; 2 μL) provided a final concentration of 0.75 mM. A 5, 5-dithiobis (2-nitrobenzoic acid) (DNTB) was added to the assay solution to give a final concentration of 0.32 mM. Absorbance was measured at OD $\lambda =$ 412 nm over a 3 min period at 25 °C on a versaMax microplate reader with SOFTMAX PRO v. 3.0 software (Molecular Devices).

Fourier transform infrared spectroscopic characterization of phosphorylated AChE adducts: Infrared spectra were collected using a Bruker IFS66/S Fourier transform infrared spectrometer (FTIR) with a Michelson interferometer. The spectrometer was purged for 10 minutes with nitrogen gas before spectral collection to decrease strong absorbances from atmospheric carbon dioxide and water vapor. Spectra were collected using a mid-infrared Globar source, a KBr beamsplitter, and a deuterated triglycine sulfate (DTGS) detector. Spectra consisted of 512 co-added scans acquired using double-sided/forward-backward mirror motion with a 10 kHz mirror velocity. Each spectrum took over seven minutes to acquire. Spectra were collected at 4 cm^{-1} resolution over the frequency range of 5200 to 500 cm^{-1}, with a 16 cm^{-1} phase resolution and a zero filling factor of 2, using a Blackman Harris three-term apodization, and

Mertz phase correction. A 16 kHz low-pass filter was used to prevent aliasing. Absorbance spectra were obtained by rationing the attenuated total reflectance (ATR) spectra of the samples to the ATR spectra of the uncoated diamond crystal.

Preparation of HRP- anti-AChE conjugate: The HRP-anti-AChE conjugate was prepared by following a modified procedure described by Graback and Gergely.[40] Briefly, HRP was activated by adding HRP (0.5 mg) in activation buffer (1 mL) containing MES (0.1 M) and NaCl (0.5 M, pH 6.0). A total of EDC (0.4 mg, final concentration $\approx$2 mM) and NHS (0.6 mg, final concentration $\approx$5 mM) were added to the activated HRP solution, and reacted for 15 minutes at room temperature. The EDC was quenched by adding 2-mercaptoethanol (1.4 μL, final concentration of 20 mM). The excess reducing agent and inactivated crosslinker were removed with a PD-10 column. The eluent was collected and concentrated to 1 mL in an ultracentrifuge tube. An amount of Anti-AChE was added at an equal molar equivalent to the HRP in the above solution, and the reaction proceeded for 2 h at room temperature. The reaction was quenched by adding hydroxylamine to a final concentration of 10 mM. Excess hydroxylamine was removed using a PD-10 column and the eluent was collected and kept at 4 °C for further use.

Preparation of QD-anti-AChE antibody conjugates: Qdot@655 antibody conjugation kit from Invitrogen was used to conjugate the anti-hAChE antibody to QDs. Before conjugation, anti-AChE from a human was purified with a gel-filtration column (Superose 12, Pharmacia-LKB) to remove surfactants and other proteins, such as bovine serum albumin (BSA). The collected eluent fractions (10 mM phosphate, 138 mM NaCl, 2.7 mM KCl, pH 7.4) were mixed and concentrated to 0.3 mL by a centrifugal filter device (Amicon Ultra-15). The concentration of anti-AChE was $\approx$0.5 mg mL^{-1}. Conjugation was performed according to the manufacturer's procedure. Anti-AChE was reduced with dithiothreitol (DTT) to expose free sulfhydryls and excess DTT was removed by size-exclusion chromatography. QDs were activated using the hetero-bifunctional crosslinker, 4-(maleimidomethyl-1cyclohexanecarboxylic acid N-hydroxysuccinimide ester (SMCC), yielding a maleimide-nanocrystal surface. Excess SMCC was removed by size-exclusion chromatography. Activated QDs were mixed with reduced anti-AChE and a coupling reaction proceeded for 1 hr. The reaction was quenched by adding β-mercaptoethanol. The produced conjugate was concentrated by ultrafiltration and purified using size-exclusion chromatography. The eluted QDs-anti-AChE conjugate was collected and then stored at 4 °C for further use.

Preparation of ZrO_2 nanoparticle-coated SPE: Before experiments, the screen printed electrode (SPE) was washed with distilled water and dried with nitrogen. ZrO_2 nanoparticles were deposited onto bare SPE in an aqueous electrolyte $ZrOCl_2$ (5.0 mM) and KCl (0.1 M) by cycling the potential between −1.1 and + 0.7 V (versus Ag/AgCl) at a scan rate of 20 mV s^{-1} for 10 consecutive scans.[36] The SPE modified with zirconia nanoparticles (ZrO_2/SPE) was rinsed with water and dried with N_2 prior to use.

Enzyme linked immunosorbent assay of phosphorylated AChE adducts: Phosphorylated AChE adduct or purified AChE (50 μL) with the desired concentration was placed in each microtiter plate well. Control experiments were performed by adding blocking buffer (50 μL, PBS containing 1% BSA) in the microplate wells. The plate was covered with an adhesive plastic and incubated overnight at 4 °C. The coating solution was then removed, and the plate washed twice by filling the wells with 200 μL PBS. The washes were removed by flicking the plate over a sink. The remaining drops were removed by patting the plate on a paper towel. The remaining protein-binding sites in the coated wells were blocked by adding 200 μL of blocking buffer per well. The plate was incubated for 2 h at room temperature. The plate was then washed twice with PBS. HRP-Anti-AChE (100 mL, 1/100) in blocking solution was added and the immunoreaction proceeded for 2 h at room temperature. The plate was then washed four times with PBS. Substrate (100 μL, TMB + H_2O_2) was added to each well and the enzyme catalyzed reaction progressed for 20 minutes at room temperature. Hydrochloric acid (100 μL, 1 M) was then added to stop the enzymatic reaction, and the plate was read on a microplate reader at λ = 450 nm.

Electrochemical immunosensing phosphorylated AChE with ZrO_2/SPE and QD labeled anti-AChE: Phosphorylated AChE solution (50 μL) at the desired concentration was aliquoted atop a ZrO_2-coated SPE surface and incubated for 1 h in a humidified chamber. The phosphorylated AChE attached SPE was then washed intensively with washing buffer (0.05 M phosphate buffer containing 0.1% w/w Tween, pH 7.4). The washing included a 1 min rinse from a washing bottle followed by a 5 min wash in a Millipore stirring cell (model 8010). The SPE was blocked for 30 min with BSA (0.5%) in phosphate buffer (0.05 M). After washing, the SPE was incubated with QD-anti-AChE (10 μL, 1/50, v/v) for 1 h in the humidified chamber, then thoroughly rinsed with PBS, and then shaken with washing buffer following the above procedure to remove the physical adsorption of QD-anti-AChE on the electrode surface. The SPE was rinsed with PBS again and dried under an N_2 stream. An aliquot of HCl (10 μL, 1 M) was dropped on the working electrode surface of the SPE to dissolve the captured QDs. The detection solution (1 M) containing 10 μg mL^{-1} Hg in acetate buffer (0.2 M, pH 4.6) was then added for electrochemical measurement. Square-wave voltammetry (SWV) measurements were performed using an in situ-plated Hg film on the SPE by a 2 min accumulation at −1.4 V. Subsequent stripping was performed after a 2-second rest period from −1.0 V to −0.5 V with a step potential of 4 mV, amplitude of 25 mV, and frequency of 15 Hz.

Safety considerations: Organophosphates (paraoxon), cadmium, and mercury are highly toxic and the wastes containing these compounds should be collected in a specific container. Skin and eye contact and accidental inhalation or ingestion should be avoided.

Acknowledgements

This work was supported by the National Institutes of Health CounterACT Program through the National Institute of Neurological Disorders and Strokes (award No. NS058161–01) and partially by CDC/NIOSH Grant R01 OH008173–01. We thank Andrea Busby for performing the Ellman assays in this study. The research described in this paper was performed at the Environmental Molecular Sciences Laboratory, a national scientific user facility sponsored by DOE's Office of Biological and Environmental Research and located at Pacific Northwest National Laboratory, which is operated by Battelle for DOE under Contract DE-AC05–76 L01830. Its contents are solely the responsibility of the authors and do not necessarily represent the official views of the federal government.

[1] T. L. Rosenberry, *Advances in Enzymology and Related Areas of Molecular Biology*, John Wiley & Sons, New York, **1975**.
[2] S. Zhang, H. Zhao, R. John, *Biosens. Bioelectron.* **2001**, *16*, 1119–1126.
[3] S. Fennouh, V. Casimiri, C. Burstein, *Biosens. Bioelectron.* **1997**, *12*, 97–104.
[4] C. Cremisini, S. Disario, J. Mela, R. Pilloton, G. Palleschi, *Anal. Chim. Acta* **1995**, *311*, 273–280.
[5] A. Guerrieri, L. Monaci, M. Quinto, F. Palmisano, *Analyst* **2002**, *127*, 5–7.
[6] R. C. Gupta, *Toxicology of Organophosphate and Carbamate Compounds*, Elsevier Academic Press, New York, **2006,** Chapter 2, pp 5.
[7] B. Goozner, L. I. Lutwick, E. Bourke, *J. Assoc. Acad. Minor. Phys.* **2002**, *13*, 14–18.
[8] M. Rosenbloom, J. B. Leikin, S. N. Vogel, Z. A. Chaudry, *Am. J. Ther.* **2002**, *9*, 5–14.
[9] http://grants.nih.gov/grants/guide/rfa-files/RFA-NS-06-004.html.
[10] W. Franz, K. Marianne, T. Horst, S. Ladislaus, *Toxicology* **2002**, *214*, 182–189.
[11] A. J. J. Ooms, C. van Dijk, *Biochem. Pharmacol.* **1966**, *15*, 1361–1377.
[12] H. L. Boter, A. J. J. Ooms, *Biochem. Pharmacol.* **1967**, *16*, 1563–1569.

[13] D. J. Ecobichon, A. M. Comeau, *Toxicol. Appl. Pharmacol.* **1973**, *24*, 92–100.
[14] M. K. Johnson, *Arch. Toxicol.* **1975**, *34*, 259–288.
[15] M. K. Johnson, P. Glynn, *Toxicol. Lett.* **1995**, *82*/83, 459–463.
[16] F. Fonnum, S. H. Sterri, P. Aas, H. Johnsen, *Fundam. Appl. Toxicol.* **1985**, *5*, S29-S38.
[17] R. M. Black, J. M. Harrison, R. W. Read, *Arch. Toxicol.* **1999**, *73*, 123–126.
[18] M. A. Sogorb, E. Vilanova, *Toxicol. Lett.* **2002**, *128*, 215–228.
[19] M. Minami, D. M. Hui, M. Katsumata, H. Inagaki, C. A. Boulet, *J. Chromatogr. B* **1997**, *695*, 237–244.
[20] G. L. Ellman, K. D. Courtney, V. Anders, R. M. Featherstone, *Biochem. Pharmacol.* **1961**, *7*, 88–95.
[21] P. Eyer, F. Worek, D. Kiderlen, G. Sinko, A. Stuglin, V. Simeon-Rudolf, E. Reiner, *Anal. Biochem.* **2003**, *312*, 224–227.
[22] F. Worek, U. Mast, D. Kiderlen, C. Diepold, P. Eyer, *Clin. Chim. Acta* **1999**, *288*, 73–90.
[23] a) D. Noort, H. P. Benschop, R. M. Black, *Toxicol. Appl. Pharmacol.* **2002**, *184*, 116–126; b) V. A. Sakkas, D. A. Lambropoulou, T. M. Sakellarides, T. A. Albanis, *Anal. Chim. Acta* **2002**, *467*, 233–243.
[24] R. M. Black, R. J. Clarke, R. W. Read, M. T. J. Reid, *J. Chromatogr. A* **1994**, *662*, 301–321.
[25] D. Noort, A. G. Hulst, H. J. M. Platenburg, M. Polhuijs, H. P. Benschop, *Arch. Toxicol.* **1998**, *72*, 671–675.
[26] R. M. Black, R. W. Read, *J. Chromatogr. A* **1997**, *759*, 79–92.
[27] M. Polhuijs, J. P. Langenberg, H. P. Benschop, *Toxicol. Appl. Pharmacol.* **1997**, *146*, 156–161.
[28] A. Fidder, D. Noort, A. G. Hulst, R. De Ruiter, M. J. van der Schans, H. P. Benschop, J. P. Langenberg, *Chem. Res. Toxicol.* **2002**, *15*, 582–590.
[29] J. A. Doorn, M. Schall, D. A. Gage, T. T. Talley, C. M. Thompson, R. J. Richardson, *Toxicol. Appl. Pharmacol.* **2001**, *176*, 73–80.
[30] D. Noort, A. G. Hulst, L. P. A. de Jong, H. P. Benschop, *Chem. Res. Toxicol.* **1999**, *12*, 715–721.
[31] K. M. George, T. Schules, L. E. Sandoval, L. L. Jennings, P. Taylor, C. M. J. Thompson, *Biol. Chem.* **2003**, *278*, 45512–45518.
[32] a) M. Cousino, T. Jarbawi, H. B. Halsall, W. R. Heineman, *Anal. Chem.* **1997**, *69*, 544 A-549 A; b). G. Liu and Y. Lin, *Talanta* **2007**, *74*, 308–317.
[33] a) J. Wang, *Small* **2005**, *1*, 1036–1043; b) J. Wang, G. Liu, Y. Lin, *Small* **2006**, *2*, 1134–1138; c) J. Wang, G. Liu, M. H. Engelhard, Y. Lin, *Anal. Chem.* **2006**, *78*, 6974–6979; d) G. Liu, J. Wang, H. Wu, Y. Lin, *Electroanalysis* **2007**, *19*, 777–785.
[34] a) G. Liu, J. Wang, H. Wu, Y. Lin, *Anal. Chem.* **2006**, *78*, 7417–7423; b) G. Liu, H. Wu, J. Wang, Y. Lin, *Small* **2006**, *2*, 1139–1143; c) G. Liu, Y. Lin, J. Wang, H. Wu, C. M. Wai, Y. Lin, *Anal. Chem.* **2007**, *79*(20),7644–7653; d) G. Liu, Y. Lin, *Anal. Chem.* **2006**, *78*(3), 835–843; e) H. Wu, G. Liu, Y. Lin, *Electrochem. Commun.* **2007**, *9*, 1573–1577.
[35] a) J. R. Fukuto, *Environ. Health Perspect.* **1990**, *87*, 245–254; b) A. Chatonnet, O. Lockridge, *Biochem. J.* **1989**, *260*, 625–634.
[36] G. Liu, Y. Lin, *Anal. Chem.* **2005**, *77*, 5894–5901.
[37] H. K. Kweon, K. Hakansson, *Anal. Chem.* **2006**, *78*, 1743–1749.
[38] L. Lin, N. S. Lawrence, S. Thongngamdee, J. Wang, Y. Lin, *Talanta* **2005**, *65*,144–148.
[39] L. Lin, S. Thongngamdee, J. Wang, Y. Lin, O. A. Sadik, S. Y. Ly, *Anal. Chim. Acta* **2005**, *535*, 9–13.
[40] Z. Grabarek, J. Gergely, *Anal. Biochem.* **1990**, *185*, 131–135.

Received: March 7, 2008
Published online: October 22, 2008

